

AD-A128 484

MECHANISM OF THERMAL DEGRADATION OF SOME
POLYPHOSPHAZENES(U) PITTSBURGH UNIV PA DEPT OF
METALLURGICAL AND MATERIALS ENGINE..
S V PEDDADA ET AL. 27 SEP 82

1/1

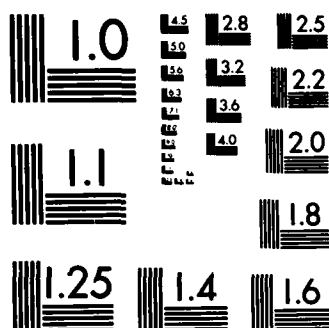
UNCLASSIFIED

F/G 11/9

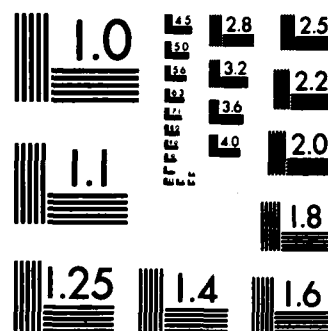
NL

END

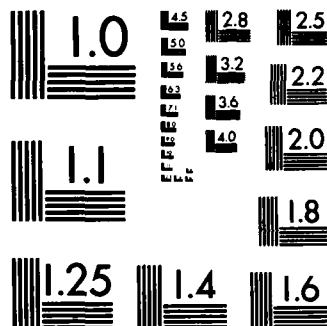
FORMED
L.F.
DTIC



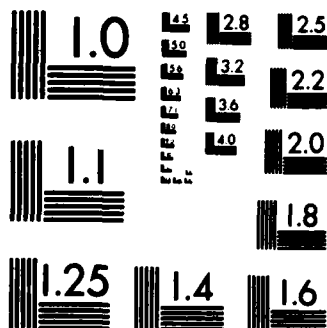
MICROCOPY RESOLUTION TEST CHART
NATIONAL BUREAU OF STANDARDS-1963-A



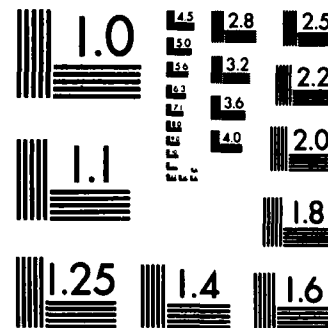
MICROCOPY RESOLUTION TEST CHART
NATIONAL BUREAU OF STANDARDS-1963-A



MICROCOPY RESOLUTION TEST CHART
NATIONAL BUREAU OF STANDARDS-1963-A

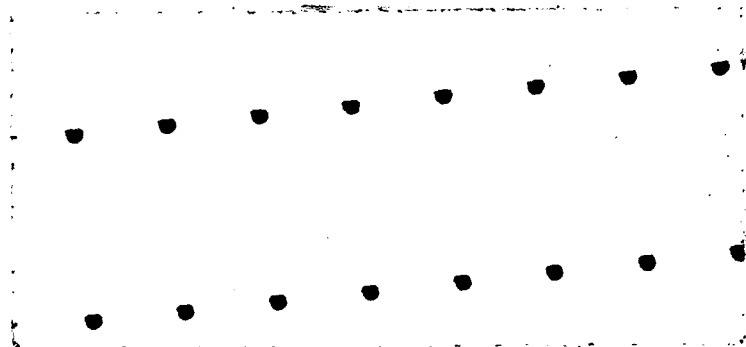


MICROCOPY RESOLUTION TEST CHART
NATIONAL BUREAU OF STANDARDS-1963-A



MICROCOPY RESOLUTION TEST CHART
NATIONAL BUREAU OF STANDARDS-1963-A

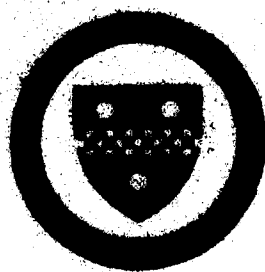
AD A120404



METALLURGICAL AND MATERIALS ENGINEERING

University of Pittsburgh
Pittsburgh, Pennsylvania 15261

DTIC
SELECTED
OCT 18 1982
H



DISTRIBUTION STATEMENT A
Approved for public release;
Distribution Unlimited

WIL FIF COPY

82 10 18 019

MECHANISM OF THERMAL DEGRADATION
OF SOME POLYPHOSPHAZENES

(12)

S. V. Peddada and J. H. Magill

Dept. of Metallurgical & Materials Engineering
University of Pittsburgh
Pittsburgh, PA 15261 U.S.A.

Submitted to Macromolecules - September, 1982

DTIC
ELECTRA
OCT 1982
H

DISTRIBUTION STATEMENT A

Approved for public release;
Distribution Unlimited

REPORT DOCUMENTATION PAGE		READ INSTRUCTIONS BEFORE COMPLETING FORM
1. REPORT NUMBER 7	2. GOVT ACCESSION NO. AD-A120404	3. RECIPIENT'S CATALOG NUMBER
4. TITLE (and Subtitle) Mechanism of Thermal Degradation of Some Polyphosphazenes		5. TYPE OF REPORT & PERIOD COVERED Interim Technical Report
		6. PERFORMING ORG. REPORT NUMBER
7. AUTHOR(s) S. V. Peddada and J. H. Magill		8. CONTRACT OR GRANT NUMBER(s) N00014-77-C-0310
9. PERFORMING ORGANIZATION NAME AND ADDRESS		10. PROGRAM ELEMENT, PROJECT, TASK AREA & WORK UNIT NUMBERS NR 356-644
11. CONTROLLING OFFICE NAME AND ADDRESS Office of Naval Research, Dept. of the Navy Arlington, VA 22217		12. REPORT DATE September 27, 1982
		13. NUMBER OF PAGES 32
14. MONITORING AGENCY NAME & ADDRESS (if different from Controlling Office)		15. SECURITY CLASS. (of this report) Unclassified
		15a. DECLASSIFICATION/DOWNGRADING SCHEDULE
16. DISTRIBUTION STATEMENT (of this Report) Unlimited Distribution		
17. DISTRIBUTION STATEMENT (of the abstract entered in Block 20, if different from Report)		
18. SUPPLEMENTARY NOTES		
19. KEY WORDS (Continue on reverse side if necessary and identify by block number) Polyphosphazenes, Thermal Degradation, Degradation kinetics and Mechanisms. Isothermal and non-isothermal thermogravimetry		
20. ABSTRACT (Continue on reverse side if necessary and identify by block number) The mechanism of degradation of poly[bis(trifluoroethoxy)phosphazene] (PBFP) and poly[bis(phenoxy)phosphazene] (PBPP) have been examined using dynamic and isothermal thermogravimetry. The dynamic experiments were made between 50° and 750°C at several heating rates from 2.5° to 80°C/min. and the isothermal measurements were made at 325°, 340°, 355° and 370°C. The polymers and their degraded residues were characterized by gel permeation chromatography, infrared spectroscopy and intrinsic viscosity.		

In PBFP, the overall activation energy for degradation (E_d) was between 23.2 (isothermal) to 26.6 (dynamic) kcal/mole. The order of reaction was 0.5 ± 0.1 . Maxima in the rates of isothermal degradation occurred between 30 and 35% weight loss. Based upon experimental results, the mode of initiation in PBFB was deduced as occurring at the chain ends. Sample molecular weight dropped rapidly with degradation in harmony with a few random breaks occurring at weak points along the main chain after the degradation has been initiated at the chain ends. Literature results on the thermal degradation of PBFP in vacuum was shown to be consistent with a terminal initiation-chain transfer mechanism.

For PBPP, dynamic thermogravimetry provided two activation energies at all levels of weight loss. Between 0% and 5% weight loss, E_d 's of 34 ± 1.5 and 29 ± 1.5 kcal/mole, and between 5% and 50% weight loss E_d 's of 37 ± 1.5 and 26 ± 1.5 kcal/mole were determined. The differential weight loss curves appeared skewed and a 25% residue was present at 600°C. Higher residues 31 to 35% were found in isothermal where an E_d of 32 kcal/mole was determined the molecular weights of degraded samples remained almost constant up to 20% degradation. A depolymerization mechanisms with some degree of cross-linking is invoked to explain this thermal degradation behaviour of the PBPP polymer.

Accession For	
NTIS GRA&I	<input checked="" type="checkbox"/>
DTIC TAB	<input type="checkbox"/>
Unannounced	<input type="checkbox"/>
Justification	
By _____	
Distribution/	
Availability Codes	
Dist	Avail & or Special
A	

OFFICE OF NAVAL RESEARCH

Contract N00014-77-C-301

Task No. NR 356-644

TECHNICAL REPORT NO. 7

Mechanism of Thermal Degradation of
Some Polyphosphazenes

by

S. V. Peddada and J. H. Magill

Prepared for Publication in Macromolecules

University of Pittsburgh
Department of Metallurgical and Materials Engineering
Pittsburgh, PA 15261

September, 1982

Reproduction in whole or in part is permitted for any purpose
of the United States Government

This document has been approved for public release and sales;
its distribution is unlimited

ABSTRACT

The mechanism of degradation of poly[bis(trifluoroethoxy)phosphazene] (PBFP) and poly[bis(phenoxy)phosphazene] (PBPP) have been examined using dynamic and isothermal thermogravimetry. The dynamic experiments were made between 50° and 750°C at several heating rates from 2.5° to 80°C/min. and the isothermal measurements were made at 325°, 340°, 355° and 370°C. The polymers and their degraded residues were characterized by gel permeation chromatography, infrared spectroscopy and intrinsic viscosity.

In PBFP, the overall activation energy for degradation (E_d) was between 23.2 (isothermal) to 26.6 (dynamic) kcal/mole. The order of reaction was 0.3 ± 0.1 . Maxima in the rates of isothermal degradation occurred between 30 and 35% weight loss. Based upon experimental results, the mode of initiation in PBFB was deduced as occurring at the chain ends. Sample molecular weight dropped rapidly with degradation in harmony with a few random breaks occurring at weak points along the main chain after the degradation has been initiated at the chain ends. Literature results on the thermal degradation of PBFP in vacuum was shown to be consistent with a terminal initiation-chain transfer mechanism.

For PBPP, dynamic thermogravimetry provided two activation energies at all levels of weight loss. Between 0% and 5% weight loss, E_d 's of 34 ± 1.5 and 29 ± 1.5 kcal/mole, and between 5% and 50% weight loss E_d 's of 37 ± 1.5 and 26 ± 1.5 kcal/mole were determined. The differential weight loss curves appeared skewed and a 25% residue was present at 600°C. Higher residues 31 to 35% were found in isothermal where an E_d of 32 kcal/mole was determined. The molecular weights of degraded samples remained almost constant up to 20% degradation. A depolymerization mechanism with some degree of crosslinking is invoked to explain thermal degradation behaviour of the PBPP polymer.

Introduction

Stable linear poly(organophosphazenes) were first synthesized in 1965 by Allcock et al.⁽¹⁾ and since then various physical properties of poly(phosphazenes), including polymerization and depolymerization have been examined. A few investigators have studied the depolymerization/degradation of poly(Phosphazenes) but the precise mechanism of thermal degradation remains unresolved.

MacCallum and Tanner⁽²⁾ performed isothermal degradation experiments in vacuum on poly[bis(phenoxy)phosphazene] (PBPP) followed by intrinsic viscosity measurements on the degradation products. They postulated a) a low temperature reaction which is probably a depolymerization equilibration reaction accompanied by another reaction at higher temperatures where other than the lower molecular weight phosphazene homologues are formed. Allen, Lewis and Todd⁽³⁾ who made dynamic thermogravimetric measurements in nitrogen at 10°C/min and isothermal measurements at 255°C, concluded that in aryloxy polymers the side groups are involved in forming crosslinks below the temperature at which the main chain degrades. From the isothermal degradation of a trifluoroethoxy-phenylphenoxy phosphazene copolymer in air at 155°C, Allen and Mortier⁽⁴⁾ noted that a decreasing stability with increasing trifluoroethoxy content was apparent. In some studies⁽²⁻⁴⁾, a systematic kinetic analysis, based upon both isothermal and dynamic thermogravimetric measurements was not performed, nor were molecular weight - weight loss data obtained.

Allcock and Cook⁽⁵⁾ investigated the thermal degradation of poly[bis(trifluoroethyl phosphazene)] (PBFP) under isothermal conditions in vacuum at temperatures between 100° and 300°C. Molecular weight measurements were carried out on the polymer residues and mass spectroscopy measurements made on the trapped volatile products. An overall degradation mechanism was proposed which qualitatively supports a random

initiation and chain unzipping mechanisms. Allcock, Moore and Cook⁽⁶⁾ studied the degradation of PBFP and concluded that the reaction proceeds by a two step process. Firstly cleavage of the main chain occurs at weak points and then cyclization depolymerization is initiated from the chain ends of the linear fragments. Allcock et al.^(5,6), obtained extensive molecular weight-weight loss data, but did not test their experimental data against theoretical depolymerization rate equations, nor did they analyse the kinetics of the degradation.

Kyker and Valaitis⁽⁷⁾ have studied the thermal degradation of a polyphosphazene containing a mixture of trifluoroethoxy and octafluoropentoxy substituents using both isothermal thermogravimetric and molecular weight measurements. These workers proposed that degradation by random scission occurred at a point in the chain followed by rapid depolymerization. Hagnauer and La Liberte⁽⁸⁾ performed isothermal degradation studies on poly[bis(m-chlorophenoxy)phosphazene] in static air and concluded that random scission took place at weak points in the chain backbone. However, they did not test for consistency between their molecular weight-weight loss data and theoretical models of degradation.

Recently Zeldin, Jo and Pearce⁽⁹⁾ degraded PBFP isothermally in vacuum, and they also performed dynamic degradation experiments. They proposed a random initiation and partial unzipping mechanism to explain the mode of degradation of PBFP. In their work, maxima in the rates of degradation of PBFP were reported as occurring at 40% weight loss. Simha, Wall and Bram⁽¹⁰⁾ modeled degradation per se, via random initiation where various zip lengths were involved. Maxima in the polymer degradation rates always occurred at or below 26% weight loss. In another study, a similar conclusion was arrived at by Boyd⁽¹¹⁾ if (a) terminal initiation occurs with chain transfer and (b) terminal initiation with some degree

of random scission takes place. These possibilities have not considered in reference 9.

In our study, the thermal degradation of PBFP and PBPP has been investigated by isothermal and dynamic thermogravimetry respectively. The appropriateness of the kinetic parameters such as overall activation energy (E_d) and order (n) so determined were confirmed by curve fitting data with theory. Molecular weight changes with degradation time were fitted to theoretical equations developed by Boyd⁽¹¹⁾. Thermal degradation of PBFP supports a mechanism of terminal initiation with some degree of scission occurring randomly at weak points along the backbone. The data of Zeldin et al.,⁽⁹⁾ have been reexamined and found to satisfy a degradation mechanism involving terminal initiation with chain transfer. The degradation of PBPP was noted to be even more complex, involving a dual mechanism, wherein depolymerization is accompanied or followed by crosslinking.

Theory. In general isothermal rate data are analyzed according to the traditional method outlined by Madorsky⁽¹²⁾. From curves of weight loss rate versus weight loss at different isothermal temperatures, the overall activation energy was determined from equation (1).

$$E_d = -2.3R [d(\log \bar{k})/d(1/T)] \quad (1)$$

where \bar{k} is the extrapolated initial rate* of weight loss, E_d is the overall activation energy for degradation, R is the gas constant and T is the absolute temperature.

A general method for determining E_d directly from weight loss - temperature data at several heating rates was presented by Flynn and Wall⁽¹³⁾. The rate of loss is given by

*Madorsky⁽¹²⁾ has shown that from isothermal measurements, an accurate value of E_d can be obtained if the residues have the same average MW and MWD (as the original sample). These conditions strictly hold only at 0% weight loss.]

$$\frac{dC}{dT} = \frac{A}{\beta} \cdot f(C) \cdot \exp \left[-\frac{E_d}{RT} \right] \quad (2)$$

where, C = fractional weight loss = $\frac{W_o - W}{W_o} = 1 - \frac{W}{W_o}$

W = sample weight at any instant

A = preexponential factor

β = heating rate

$f(C) = (1-C)^n$ is a function of the fractional sample weight.

n = order of the reaction.

By the method of separation of variables and integration of equation

(2) it follows that

$$\log \left[-\frac{(1-C)^{1-n}-1}{1-n} \right] = \log \left(\frac{A E_d}{R} \right) - \log \beta - 2.315 - 0.457 \frac{E_d}{RT} \quad (3)$$

when $n \neq 1$ or

$$\log [-\ln (1-C)] = \log \left(\frac{A E_d}{R} \right) - \log \beta - 2.315 - 0.457 \frac{E_d}{RT} \quad (4)$$

when $n = 1$

At constant weight loss (fixed C) for several heating rates, a plot of \log

$(\beta) (=dT/dt)$ versus $1/T$ exhibits a slope of

$$\frac{d(\log \beta)}{d(1/T)} = -0.457 \frac{E_d}{R} \text{ or } E_d = -4.35 \frac{d \log \beta}{d(1/T)} \quad (5)$$

Equation (5) has been used to determine the magnitude of E_d from dynamic weight loss data.

Reich and Stivala⁽¹⁴⁾ outlines another technique whereby values of fractional weight loss (C) and corresponding temperatures (T) are used to calculate E_d 's for arbitrary E_d values so obtained were plotted against respective n values and the region bounded by the interesting curves was used to simultaneously estimate E_d and n , hence A . It is implicitly assumed here that the mechanism of degradation is

invariant during the reaction. The parameters so obtained were then used to calculate a theoretical (1-C) vs. T curve, for comparison with the experimental one.

Experimental Section

1. Materials: Characterized poly[bis(trifluoroethoxy)phosphazene], PBFP and poly[bis(phenoxy)phosphazene], PBPP used in this investigation were kindly provided by Dr. G. L. Hagnauer of Army Materials and Mechanics Research Center, Watertown, MA.

2. Thermogravimetry (TG): The dynamic and isothermal thermogravimetric experiments were performed using a Perkin-Elmer, TGS-2, with a first derivative controller unit attached in series with a System-4 microprocessor controller and X-Y₁-Y₂ recorder. All samples were heated at 50°C for hours in vacuum and rid them of any low molecular weight species. Dynamic thermogravimetric measurements were made at heating rates of 2.5°, 5°, 10°, 20°, 40° and 80°C/min., respectively between 50° and 750°C with a helium gas flow of 160 cm³/min. Sample weights were in the range of 3 to 5 mg. At least two reproducible runs were obtained for each condition.

Isothermal thermogravimetric measurements were made at 325°, 340°, 355° and 370°C for sample weights of 3 to 5 mg with a helium flow rate of 160 cm³/min. In these measurements the furnace was preheated to the selected isothermal temperature, and then runs were initiated by quickly raising the preheated furnace assembly around the sample, which rapidly reached the degradation temperature. The decrease in sample weight was recorded as a function of time. Measurements were checked for reproducibility.

3. Gel Permeation Measurement (G.P.C.). Measurements were made on PBFP to determine the change in molecular weight with degradation time. Results were compared with the intrinsic viscosity measurements on the same samples. A Waters - 1600, with Bondagel packed columns, was employed using THF as the solvent phase.

In addition, sample residues at different extents of degradation at 355°C were used for intrinsic viscosity, and infrared measurements.

4. Molecular weight measurements: Intrinsic viscosity (η) measurements using a Cannon-Ubbelohde viscometer at $25^\circ \pm 0.01^\circ\text{C}$, were made on the original PBFP and PBPP samples and their residues obtained at 355°C. Acetone was the solvent for PBFP and tetrachloroethane was used for PBPP. At each concentration, at least three efflux times were recorded at flow times where kinetic energy corrections were not required. The isothermal TG data was analysed using a computerized curve digitizer. The rate of weight loss curves based on original sample weight and residue were computed and plotted as illustrated (for example) in Figure 2. Measurements were made on PBPP and its residues on a Waters ALC/GPC-244, using DuPont Bimodal (60\AA and 1000\AA)-silanized columns using THF as the mobile phase. These measurements were kindly provided by Dr. G. L. Hagnauer for some of our samples.

Results and Discussion

A. Poly[bis(trifluoroethoxy)phosphazene], PBFP. The fractional weight loss (fractional volatilization) versus time curves from the isothermal degradation of PBFP are presented in Figure 1. The corresponding differential weight loss curves, Figure 2, exhibits maxima in the rates between 30 and 35% weight loss; i.e. greater than the 26% predicted by Simha et al.,⁽¹⁰⁾ and by Boyd⁽¹¹⁾ for only random initiated degradation. Note too that Zeldin et al.⁽⁹⁾, observed maxima at approximately 40% weight loss. These results suggest that thermal initiation in PBFP takes place from chain ends in contrast to random scission initiation. The rates of weight loss, based upon polymer residue, are plotted in Figure 3, and from such data the extrapolated initial rates (\bar{k}) were determined. An activation energy (E_d) of 23.0 kcal/mole was determined using equation (1).

Experimental rate curves were compared with the calculated curves based upon zero order kinetics, and fairly good agreement was found, suggesting a pseudo zero order reaction for this polyphosphazene.

Using the method of Flynn and Wall⁽¹³⁾, an activation energy value of 26.6 kcal/mole was determined (equation (5)) from the dynamic degradation data of PBFP in helium. Dynamic thermogravimetric data analyzed using the technique outlined by Reich and Stivala, provided the E_d , n and A values for PBFB degradation of 5°, 10° and 20°C/min. The average of these parameters from the three different heating rates are summarized in Table 1.

TABLE 1

AVERAGE KINETIC PARAMETERS FROM DYNAMIC THERMOGRAVIMETRY

% Weight Loss	E_d (kcal/mole)	n	A (l/min)
0-20	16 ± 0.4	0.3 ± 0.1	2.5×10^4
Beyond 20	23.4 ± 1.5	0.3 ± 0.1	4.5×10^6

With the parameters listed in Table 1 and Equation (3), the temperatures of degradation were calculated at different weight loss levels, so providing a degradation curve for comparison with the experimental results. Figure 4 illustrates the agreement obtained for a heating rate of 10°C/min. Heating rates of 5° and 20°C/min provide equally good agreement.

The E_d values determined from isothermal thermogravimetry were ~ 23.2 kcal/mole. From the dynamic TG method of Flynn and Wall values ~ 26.6 kcal/mole resulted. The method of Reich and Stivala gave ~ 23.4 kcal/mole above 20% weight loss. They do compared favorably. However a low E_d value (~ 16 kcal/mole) also was obtained by the latter technique below 20% weight loss. This is surprising in view of the fact that the weight loss curves (not shown) do not indicate a dual reaction mechanism as they are superposable by a lateral shift, nor do the

differential weight loss curves display a shoulder.

Generally, low E_d , values, typically ≤ 30 kcal/mole, are more consistent with a chain-end initiated degradation mechanism. In case of the thermal depolymerization of poly(dichlorophosphazene) $E_d = 22-26$ kcal/mole,⁽¹⁵⁾ or for the chain-end unzipping mechanism of PMMA⁽¹⁶⁾ E_d values less than 30 kcal/mole are found. The lower activation energy is needed in the initiation degradation step as opposed to pure random scission, occurring other than at chain weak points. This is a further reason why we conclude that the mode of initiation in PBFP is more likely to occur at chain ends and not by random scission.

Although we have some reservations about the order of the reaction when the degradation process(es), is complex and molecular weight distribution broad, the magnitude of "n" is still significant. MacCallum⁽¹⁷⁾, in his analysis of the kinetics of polymer degradation, has shown that for a randomly initiated degradation process, the reaction order with respect to the sample weight lies between one and two, whereas for end initiated degradation reaction the order is in the range of zero to one. From our isothermal measurements we presume that the reaction follows pseudo zero order kinetics and from the dynamic TG measurements we obtain a value of 0.3 which is again consistent with chain end initiated kinetics.

The intrinsic viscosity in acetone at $25 \pm 0.1^\circ\text{C}$ of PBFP starting materials and samples degraded by 2, 4 and 10% are summarized in Table 2.

TABLE 2
MOLECULAR WEIGHT OF PBFP

% Weight loss	Time(min)	$[\eta]$ (dl/g)	$[\eta]/[\eta]_0$	\bar{M}_n^*	$\bar{M}_n/\bar{M}_{n,0}$
0	0	0.284	1	49,490	1
2	1.52	0.1411	0.5	19,730	0.4
4	3.2	0.1216	0.43	16,210	0.33
10	7.2	0.0944	0.33	11,615	0.235

*The \bar{M}_n values have been determined following Zeldin et al. (see ref. 9).

The rapid decrease in molecular weight with degradation has been noted for thermal degradation initiated at chain ends⁽¹¹⁾ in two instances, namely:

- 1) terminal initiation with chain transfer, and
- 2) terminal initiation with some degree of random scission.

The most clear-cut distinction may in principle be drawn between transfer and random scission from the molecular weight change of the polymer with degradation. Boyd⁽¹¹⁾ has shown that if the degradation is by random scission then equation (6) holds:

$$\frac{1}{\bar{M}_n} - \frac{1}{\bar{M}_{n,0}} = k_r t \quad (6)$$

whereas if chain transfer is responsible for the rapid drop in molecular weight, then equation (7) applies

$$\frac{1}{\sqrt{\bar{M}_n}} - \frac{1}{\sqrt{\bar{M}_{n,0}}} = k_c t \quad (7)$$

A constant N or N' can be added to the right hand side of equations (6) and (7) respectively to account for the presence of weak links⁽¹⁸⁾. However in the absence of such defects, a plot of $1/\bar{M}_n$ vs. t (see Figure 5b) or $1/\sqrt{\bar{M}_n}$ vs. t (see Figure 5a) should yield a straight line passing through the origin. At short times, we note that both of these plots exhibit nonlinear behavior in line with the weak link concept. If weak links are absent, plots of $(\frac{1}{\bar{M}_n} - \frac{1}{\bar{M}_{n,0}})$ vs. t (Figure 5c) or $(\frac{1}{\sqrt{\bar{M}_n}} - \frac{1}{\sqrt{\bar{M}_{n,0}}})$ vs. t (Figure 5d) should also pass

through the origin, but they do not. The linear portion of these plots (5c, 5d) intercepts the ordinate axis, as in accord with other plots dealing with poly(phosphazenes)^(7,8), or where weak links⁽¹⁸⁾ are suspected in other polymer

backbones. If weakpoints are randomly distributed, then the sharp drop in molecular weight initially is attributed to random scission at these defects following thermal initiation at the chain ends. The E_d values ~ 23 to 26 kcal/mole are consistent with this picture since purely random scission involves higher activation energies.

The rapid decline in molecular weight of PBFP initially (<1.5 min) is very important mechanistically, but the changes which occur beyond this time (Table 2) are noteworthy too. Analyses of the data according to equations (6) and (7) both yield straight lines compounding the difficulties of differentiation between transfer and random scission processes. Indeed both mechanisms may be operative here. From an analytical viewpoint, no new chemical species were found by infrared spectrum since this spectrum was identical to that of the original polymer indicating that PBFP essentially degrades by splitting of the main chain. It appears then that the thermal degradation of PBFP in our work involves thermal initiation - followed by random scission at weak points.

Zeldin et al.⁽⁹⁾ from the isothermal degradation of PBFP in vacuum concluded that PBFP degraded via a random scission and partial unzipping mechanism. However their observations appear inconsistent with random initiation^(10,11,17), and specifically criteria such as:

- (a) maxima in the rate of weight loss at 40% approximately,
 - (b) order of reaction, $n = 0.8$
- and (c) relatively high values for E_d (see p. 12 for an explanation).

The molecular weight - weight loss data in Table 3 indicate a rapid drop in molecular weight.

TABLE 3

Molecular Weight Data for PBFP

w/w ₀	1.0	0.9	0.86	0.75	0.71	0.65	0.35
\bar{M}_n	305,000	61,500	46,400	20,600	15,400	13,900	12,700
\bar{DP}	1255	253	191	85	63	57	52
\bar{DP}/\bar{DP}_0	1	0.207	0.152	0.068	0.050	0.045	0.041

Once degradation is initiated at chain ends, the rapid drop in molecular weight may arise through chain transfer or via limited but random scissions. Figure 6(a,b) is a plot of $1/\bar{M}_n$ and $1/\sqrt{\bar{M}_n}$ versus time[†], where in Figure 6a the plot of $1/\sqrt{\bar{M}_n}$ versus time yields a straight line, favoring a chain transfer mechanism. The plot of $(\frac{1}{\sqrt{\bar{M}_n}} - \frac{1}{\sqrt{\bar{M}_{n,0}}})$ versus time (Figure 6c) is linear passing through the origin as expected.

Since Zeldin et al⁽⁹⁾ obtained higher E_d values 45 kcal/mole (isothermal) and 49 kcal/mole (dynamic) there may exist intrinsic sample differences between their material and that employed in our work. The discrepancy of 20 kcal/mole approximately in overall E_d 's may be explained by an activation energy for chain transfer of this magnitude. However the difference in the maxima of the rate of weight loss and the value of the order of reaction tend to support our proposed mechanism even though

- (i) terminal initiation followed by chain transfer (our analysis of their data)
- and (ii) random chain scissions coupled with partial chain unzipping

[†]Although the molecular weight-weight loss data were obtained from thermolysis at $350^\circ \pm 2^\circ\text{C}$ in vacuum, weight loss-time (isothermal degradation) data were obtained by degradation in vacuum at 355°C . Still, the MW-time results plotted in Figure (6) provide a good first approximation.

qualitatively indicates the same rapid decrease in molecular weight with weight loss or time. It is also important to point out here that the mechanism proposed by us for our PBFP material (terminal initiation coupled with limited breaks at defect regions of the chain) intrinsically shows the same reduction in molecular weights.

Based upon a terminal initiation - chain transfer mechanism, Boyd⁽¹¹⁾ developed an equation for the rate of weight loss,

$$\frac{1}{W} \frac{dW}{dt} = -k_E [-\sigma^{\circ} n^{\circ} \bar{n}^{1/2} + 1 + \bar{\gamma}] / [1 + \bar{n} \bar{\gamma} (n^{\circ} \gamma^{\circ})]$$

where,

W = total # of repeat units in the sample; when multiplied by the molecular weight of a repeat unit (m_0) it is the sample weight.

k_E = rate constant for end group initiation

x = number average degree of polymerization

$\bar{n} = n/n^{\circ}$

γ = reciprocal average zip length

$\bar{\gamma} = \gamma/\gamma^{\circ}$

σ° = transfer parameter

superscript \circ indicates initial values.

Using Boyd's approach, and making the assumption that the zip-length is comparatively long, we are able to derive the following simplifying equation, relating fractional weight and degree of polymerization

$$\ln\left(\frac{W}{W_0}\right) = \frac{-2 \bar{\gamma} [1 + \sigma^{\circ} x^{\circ}/2]}{(\sigma^{\circ} n^{\circ}) (x^{\circ} \gamma^{\circ})} \cdot \left(\frac{1}{\bar{x}} - 1\right) \quad (9)$$

Applying this equation a good agreement between experimental and predicted fractional molecular weights as a function of weight loss is obtained (see Figure 7). We therefore conclude that there is significant evidence in favor of a thermal initiation-chain transfer mechanism to explain the degradation behavior of PBFP.

b) Poly[bis(phenoxy)phosphazene], PBPP

The dynamic thermogravimetric data expressed as fractional weight loss - temperature data for PBPP in helium are plotted in Figure 8. The curves are complex and not superposable via lateral shifting. The differential weight loss curves exhibit distinct shoulders suggesting that more than one mechanism is involved. Two activation energies corresponding to two mechanisms, were found (ref. Figure 9) when data were analysed according to Flynn and Wall⁽¹³⁾. Up to 5% degradation, E_d 's of 29 ± 1.5 and 34 ± 1.5 kcal/mole were obtained. Between 5 to 50% weight loss, E_d 's of 26 ± 1.5 and 37 ± 1.5 kcal/mole were derived. The higher E_d 's corresponds to the lower heating rate (below $10^\circ/\text{min.}$) and the lower E_d arises above this rate. Residue levels about 25% and 33% corresponding to dynamic and isothermal test conditions respectively. Compared with PBFP values ($\sim 3\%$) obtained under similar environmental conditions, these levels signify that crosslinking is operative and that the side group chemistry is important. It is gratifying to see that an E_d of 31 kcal/mole was determined from our isothermal analysis of rates of volatilization of PBPP in helium in good agreement with results obtained from dynamic measurements.

Typical isothermal degradation rates (Figure 10) exhibit maxima around 20% volatilization (weight loss) after which the rate falls to 55% approximately, but reaching zero change in weight about the 70% level. Contrast for example, the PBFP results (Figure 3) where little or no weight loss stabilization occurs (i.e. no cross-linking reaction takes place). Elsewhere it is known that crosslinking enhances thermal stability since the depolymerization tends to be "blocked" by crosslinks.

In Figure 11 and 12 at 300° and 400°C respectively literature data^(20,21) of weight loss rates (based upon residue) as a function of sample volatilized are calculated and represented by curve A. In both figures this curve resembles closely the degradation pattern of PBPP above 340°C . The results of Figure 11

have been ascribed to crosslinking during the thermal degradation of poly (propyleneoxide). In Figure 12, the trifunctional poly(trivinylbenzene)²¹ is undoubtedly associated with a crosslinking mechanism which shows a striking parallel with PBPP.

Supporting evidence for degradation with crosslinking comes from GPC data of PBPP in Table 4. The molecular weights are relative, since polystyrene standards only were used for calibration, but the MW ratios are significant for comparison of chain lengths changes during degradation even though these are minor up to 20% weight loss. Note too that degraded samples only dissolved with difficulty in tetrachloroethane at 120°C.

TABLE 4

MOLECULAR WEIGHT DATA FOR PBPP

% Weight Loss	0	1.2	4.2	10.1	20
$M_w \times 10^5$	6.6	6.8	6.2	7.6	7.9
$\bar{M}_w/\bar{M}_{w,0}$	1.00	1.03	0.94	1.15	1.2

The infrared spectrum of the original and the degraded samples up to 10% and even at 42% weight loss exhibit no significant changes in spectral features. This evidence suggests that PBPP, like PBFP, essentially degraded via backbone breakdown as opposite to side group splittings. P-O-P band is expected between 870 and 1000 cm^{-1} if (see schematic in Figure 13) crosslinking occurs. However the band is not observed since it is overlapped by the stronger P-OC₆H₅ peak at 855-994 cm^{-1} . Still, there is support for a dual degradation mechanism in PBPP involving (i) a depolymerization stage which accounts for the observed weight loss and (ii) a crosslinking reaction relating to the high residue level in degraded samples.

Overall, the difficulties associated with this work are obvious. Narrow molecular weight specimens are essential to obtain a definitive understanding of physical properties of PBPP and other polyphosphazenes. On the theoretical side consideration must be given to the role of crosslinking in order to extend and test the consistency of kinetics with models of polymer degradation.

CONCLUSIONS

1. The mode of initiation in PBFP occurs at chain ends; afterwards further breakdown of the chain takes place by limited random scission:
 - a. At weak points along the chain (one sample), and by
 - b. Chain transfer (our analysis of the data of Zeldin et al⁽⁹⁾).
2. The thermal degradation behaviour of PBPP occurs by depolymerization with crosslinking which increases with the extend of degradation finally resulting in an insoluble residue.

Acknowledgements

Support from the Office of Naval Research Contract # ONR 356-644 is gratefully acknowledged. Sincere thanks are due especially to Dr. G. L. Hagnauer of the Army Materials and Mechanics Research Center. Gratitude is also expressed to W. Pingatore and Dr. E. Casassa (Carnegie University) for infrared and G.P.C. facilities.

BIBLIOGRAPHY

1. H. R. Allcock and R. L. Kugel, J. of American Chemical Society, 1965, 87, 4216.
2. J. R. MacCallum and J. Tanner, Journal of Macromolecular Science-Chemistry, A 4(2), 481 (1970).
3. G. Allen, C. J. Lewis and S. M. Todd, Polymer, 11, 42 (1970).
4. G. Allen and R. M. Mortier, Polymer, 13, 253 (1972).
5. H. R. Allcock, W. J. Cook, Macromolecules, 7, 284 (1974).
6. H. R. Allcock, G. Y. Moore and W. J. Cook, Macromolecules, 7, 571 (1974).
7. G. S. Kyker and J. K. Valaitis, Advances in Chemistry Series, "Stabilization and Degradation of Polymers", D. L. Allara and W. L. Hawkins, Eds., 169, 293 (1978).
8. G. L. Hagnauer and B. R. LaLiberte, Journal of Applied Polymer Science, 20, 3073 (1976).
9. M. Zeldin, W. H. Jo and E. M. Pearce, Macromolecules, 13, 1163 (1980).
10. R. Simha, L. A. Wall and J. Bram, J. of Chemical Physics, 29, 894 (1958).
11. R. H. Boyd, "Thermal Stability of Polymers", R. T. Conley ed., pp. 47-89(1980).
12. S. Weeks and A. V. Astin eds., "Polymer Degradation Mechanisms," (Washington DC.: United States National Bureau of Standards Circular #525) 221 (1953).
13. J. H. Flynn and L. A. Wall, Journal of Research of the National Bureau of Standards, 70A, 487 (1966).
14. L. Reich and S. S. Stivala, Thermochimica Acta, 24, 9 (1978).
15. H. R. Allcock, "Phosphorus Nitrogen Compounds" (New York: Academic Press), pp. 337-383 (1972).
16. D. M. Gardner and K. Fraenkel, Journal of the American Chemical Society, 78, 3279 (1956).
17. J. R. MacCallum, European Polymer Journal, 2, 413 (1966).
18. G. G. Cameron and J. R. MacCallum, Reviews in Macromolecular Chemistry, G. B. Butler and R. F. O'Driscoll, Eds., Ch. 8, Marcel Dekker, New York, 1967.
19. H. F. Mark and E. H. Immergut eds., Thermal Degradation of Organic Polymers," (New York: Interscience Publishers, 1964).

20. S. L. Madorsky and S. Strauss, J. of Polymer Science, 36, 183 (1959).
21. S. L. Madorsky and S. Strauss, J. of Research of the National Bureau of Standards, 63A, 261 (1959).
22. H. H. G. Jellinek, "Degradation of Vinyl Polymers" (New York: Academic Press, 1955).
23. N. Grassie, "Chemistry of High Polymer Degradation Processes" (London: Butterworths Scientific Publications, 1956).
24. R. Simha and L. A. Wall, Journal of Physical Chemistry, 56, 707 (1952).

FIGURE LEGENDS

- Figure 1. Fractional weight loss (w/w_0) versus time (min.) for the isothermal degradation of PBFP in helium at A: 325°C; B: 340°C; C: 355°C; D: 370°C. Helium flow rate was 160 cm³/min.
- Figure 2. Isothermal weight loss rate (min⁻¹) versus fractional conversion (w/w_0) for the degradation of PBFP in helium at A: 325°C; B: 340°C; C: 355°C; D: 370°C. Dotted vertical lines denote a 26% conversion level. Data were computer digitized from thermogravimetric curves of the type shown in Figure 1.
- Figure 3. Rate of weight loss data (min⁻¹) based upon residue fraction versus fractional conversion for the isothermal degradation of PBFP in helium (150 cm³/min flow rate) at A: 325°C; B: 340°C; C: 355°C, and D: 370°C respectively. Data was computer digitized and plotted.
- Figure 4. Experimental vs. calculated fractional weight loss (1-C) curves as a function of temperature (°C) for the degradation of PBFP at 10°/min.
- Figure 5. Inverse molecular weight functions versus time (t, min.) for PBFP samples. Symbols denote the appropriate ordinate function
 (a) $M^{-1/2}$, (b) M_n^{-1} (c) $(\frac{1}{M_n} - \frac{1}{M_{n,0}})10^5$, (d) $(\frac{1}{\sqrt{M_n}} - \frac{1}{\sqrt{M_{n,0}}})10^3$
- Figure 6. Inverse molecular weight functions versus time (t, min.) for PBFP data (ref. 9). Symbols denote appropriate ordinate function plotted
 (a) $M_n^{-1/2}$, (b) M_n^{-1} , (c) $(\frac{1}{\sqrt{M_n}} - \frac{1}{\sqrt{M_{n,0}}})10^3$, (d) $(\frac{1}{M_n} - \frac{1}{M_{n,0}})10^5$
- Figure 7. Relative molecular weight fraction ($\overline{DP}/\overline{DP}_0$) versus % weight loss (from ref. 9).
- Figure 8. Percent weight loss (1-C) versus temperature (°C) for PBPP specimens at different heating rates (°C/min) from 2.5 to 80°C/min. in helium.
- Figure 9. Long rate of heating β (°C/min.) versus reciprocal temperature (K⁻¹) for the degradation of PBPP in helium for conversion levels: A 2.5%; B 5%; C 10%; D. 20%; E. 30%; F 50%.
- Figure 10. Rate of weight loss (min⁻¹) (based on residue) versus fractional conversion (abscissa) for isothermal degradation of PBPP in helium at: A 325°C; B 340°C; C 355°C; D 370°C. Data was computer digitized and plotted.
- Figure 11. Rate of volatilization of isotactic polypropyleneoxide, (wt.% sample/min) versus amount volatilized, % (wt.%) at 285°, 290°, 295° and 300°C respectively (from ref. 20). Curve A is calculated from rate data (300°C) and represents the rate of weight loss (based on residue) as a function of sample volatilized. (Figure reproduced in part by permission).

Figure 12. Rate of volatilization (wt. % per min.) of poly(trivinylbenzene) as a function of sample volatilized (wt. %) at 394°, 420, 430, and 440°C respectively (ref. 20). Curve A has been calculated from rate data at 440°C and depicts the rate of weight loss (based upon residue) as a function of sample volatilized (wt. %) (Figure reproduced in part by permission).

Figure 13. Schematic illustration of crosslinking in PBPP.

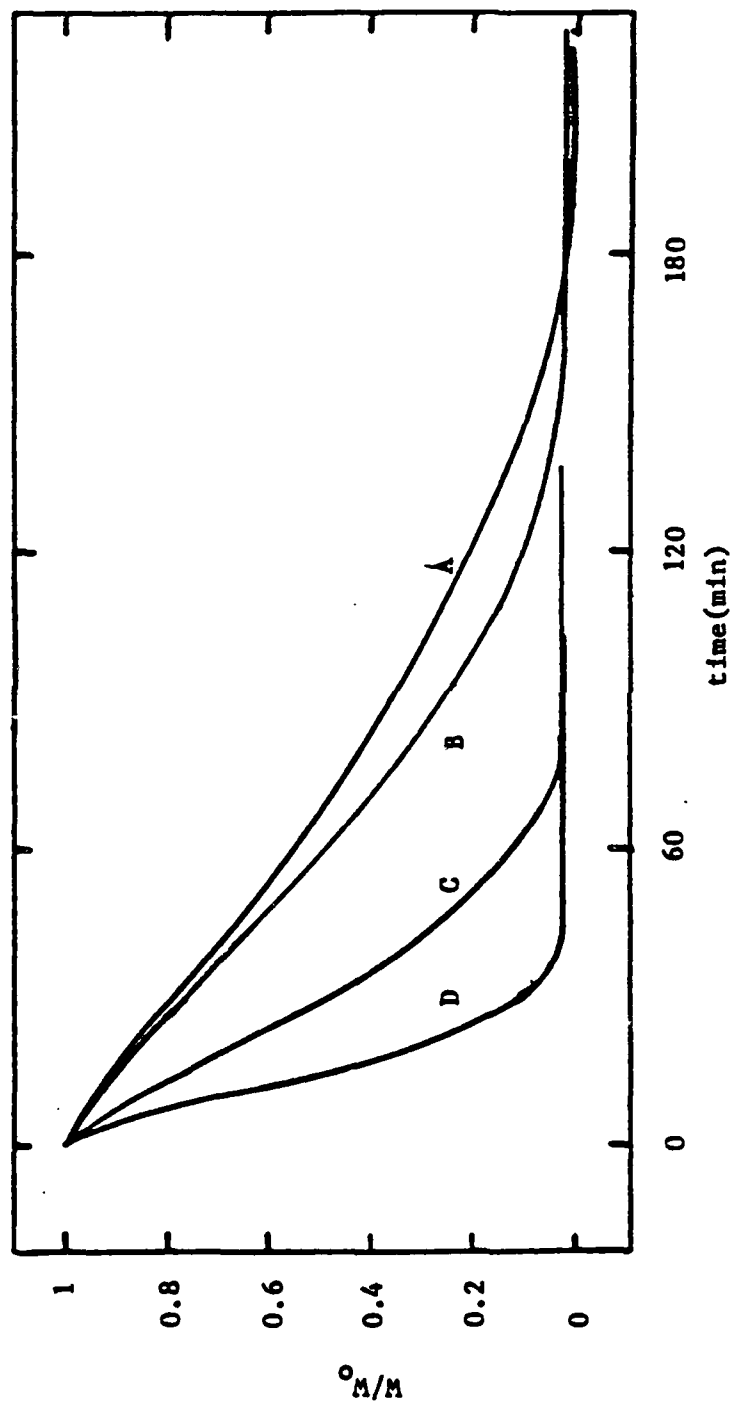


Figure 1. Fractional weight loss (w/w_0) versus time (min.) for the isothermal degradation of PBFP in helium at A: 325°C; B: 340°C; C: 355°C; D: 370°C. Helium flow rate was 160 cm³/min.

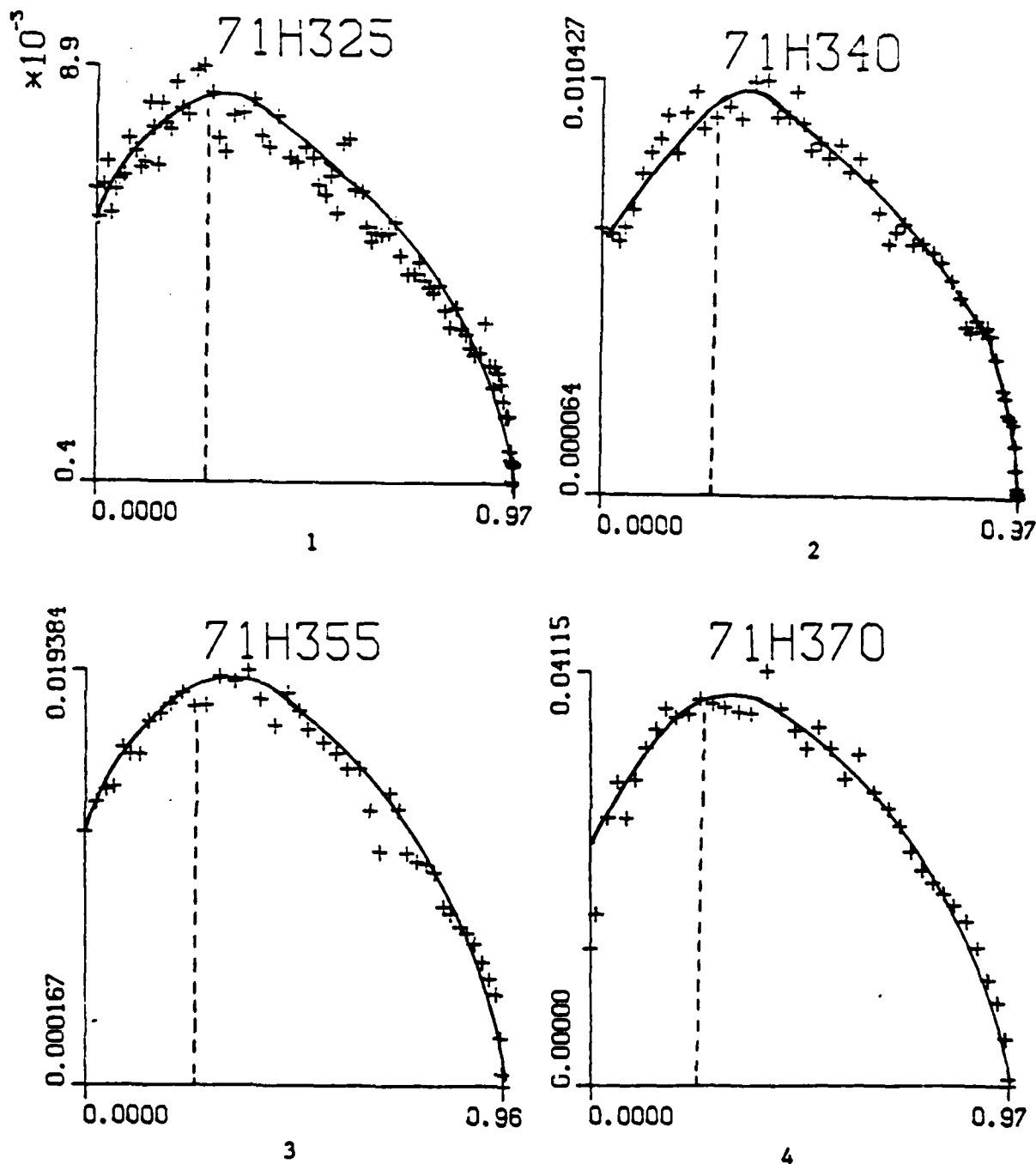


Figure 2. Isothermal weight loss rate (min⁻¹) versus fractional conversion (w/w₀) for the degradation of PBFP in helium at A: 325°C; B: 340°C; C: 355°C; D: 370°C. Dotted vertical lines denote a 26% conversion level. Data were computer digitized from thermogravimetric curves of the type shown in Figure 1.

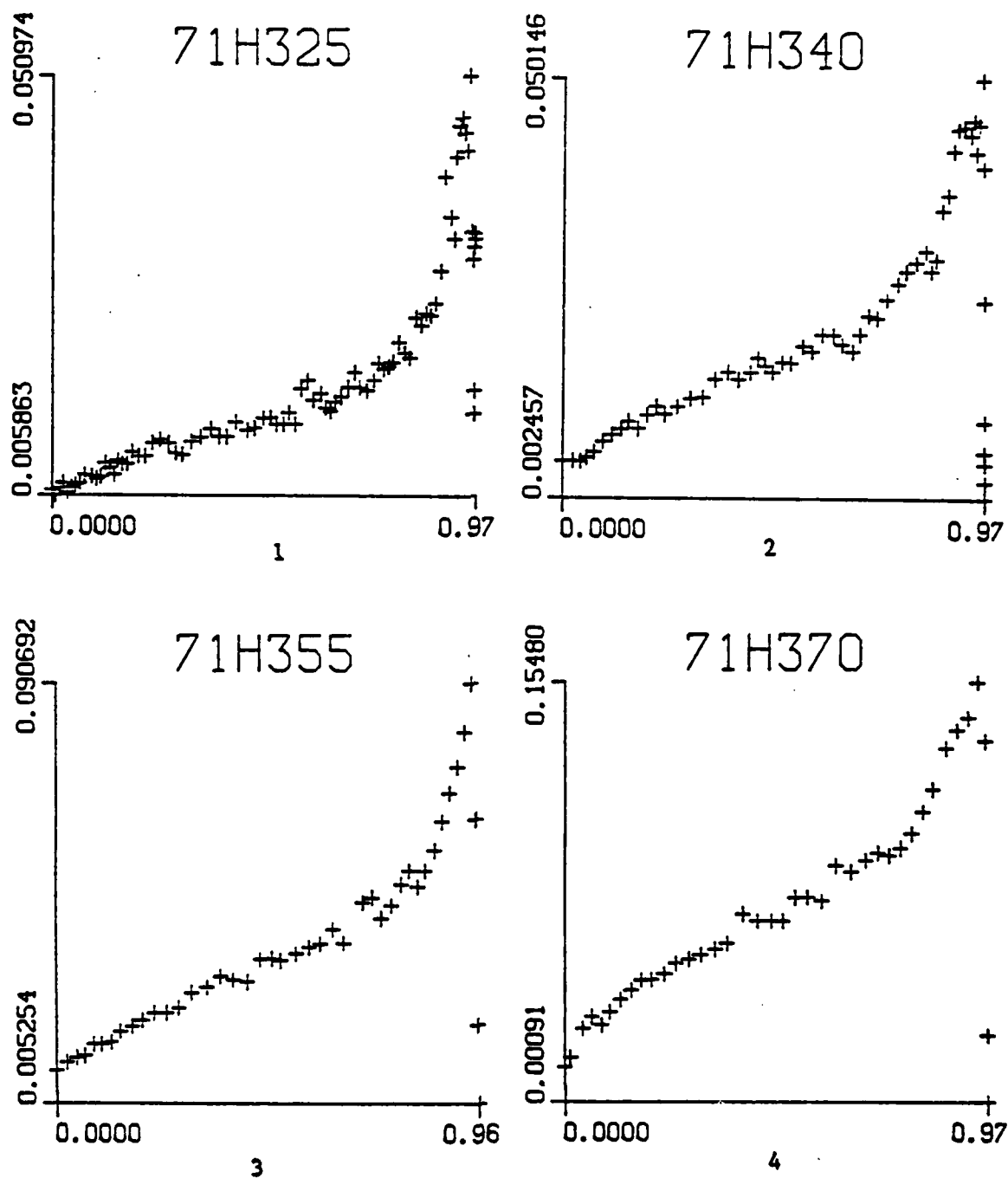


Figure 3. Rate of weight loss data (min⁻¹) based upon residue fraction versus fractional conversion for the isothermal degradation of PBFP in helium (150 cm³/min flow rate) at A: 325°C; B: 340°C; C: 355°C, and D: 370°C respectively. Data was computer digitized and plotted.

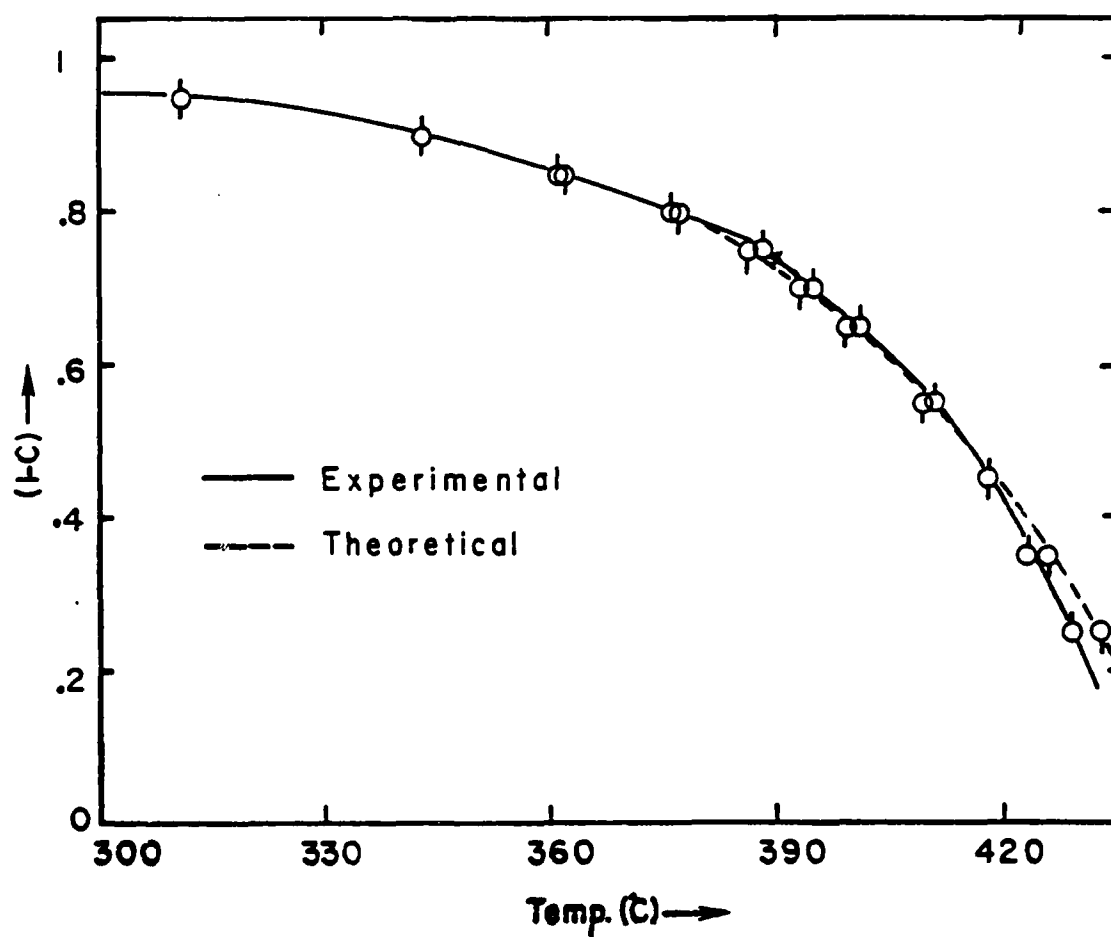


Figure 4. Experimental vs. calculated fractional weight loss $(1-C)$ curves as a function of temperature ($^\circ\text{C}$) for the degradation of PBFP at $10^\circ/\text{min}$.

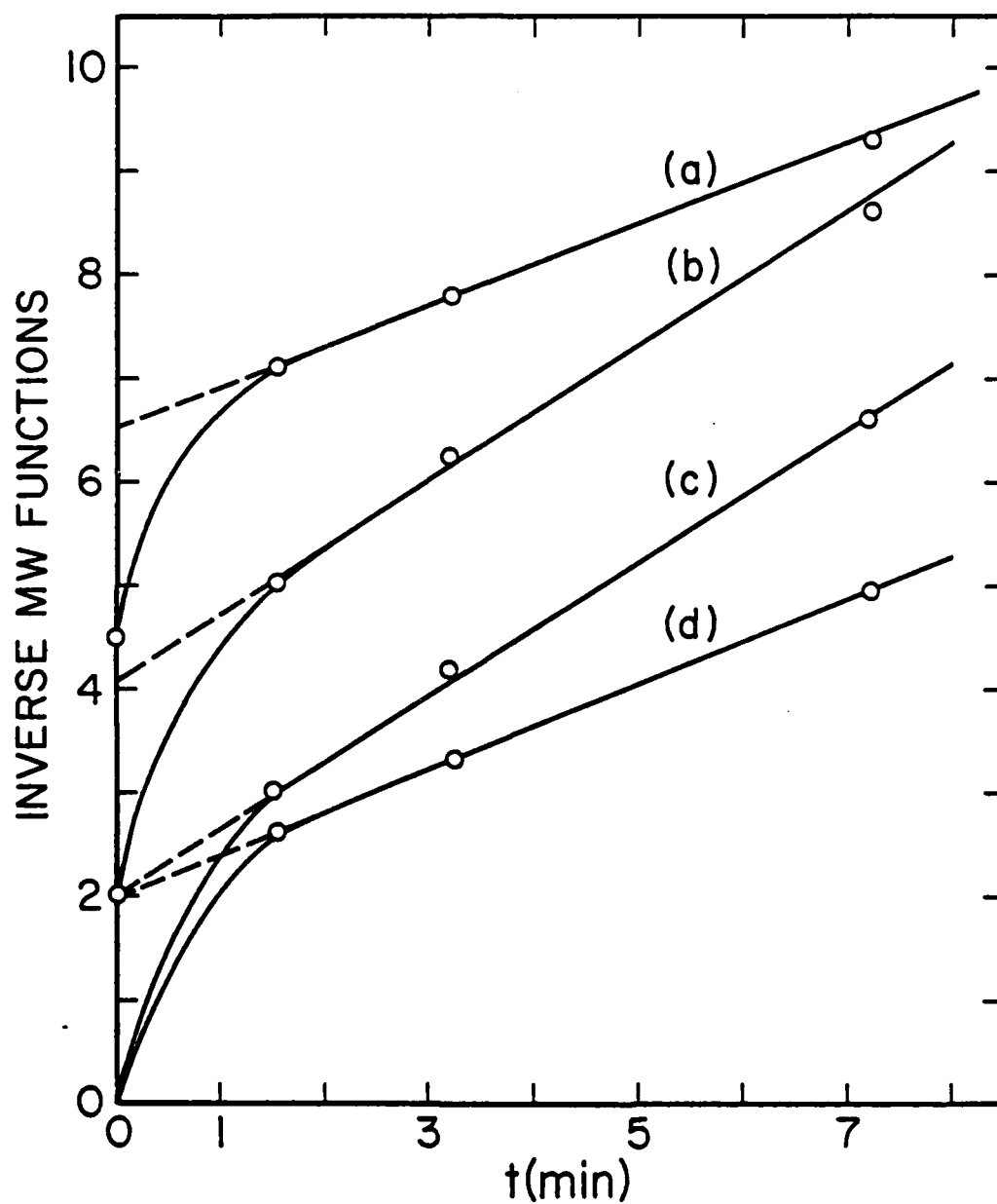


Figure 5. Inverse molecular weight functions versus time (t , min.) for PBFP samples. Symbols denote the appropriate ordinate function

(a) $M^{-1/2}$, (b) M_n^{-1} (c) $(\frac{1}{M_n} - \frac{1}{M_{n,o}}) 10^5$, (d) $(\frac{1}{\sqrt{M_n}} - \frac{1}{\sqrt{M_{n,o}}}) 10^3$

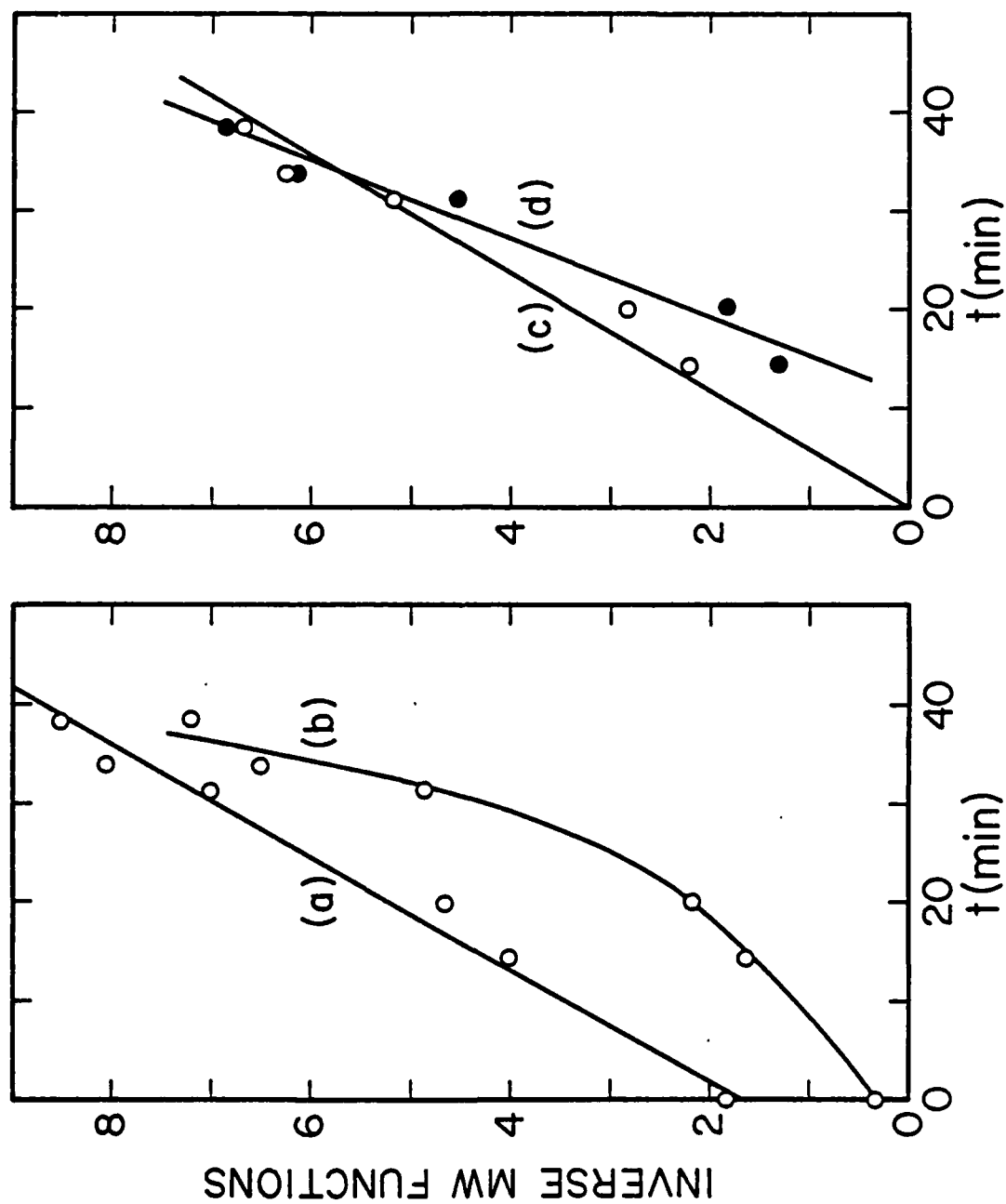


Figure 6. Inverse molecular weight functions versus time (t , min.) for PBFP data (ref. 9). Symbols denote appropriate ordinate function plotted (a) $M_n^{-1/2}$, (b) $M_n^{-1} (1 - \frac{1}{10^3} \frac{1}{M_n})$, (c) M_n^{-1} , (d) $(\frac{1}{M_n} - \frac{1}{M_0}) 10^5$.

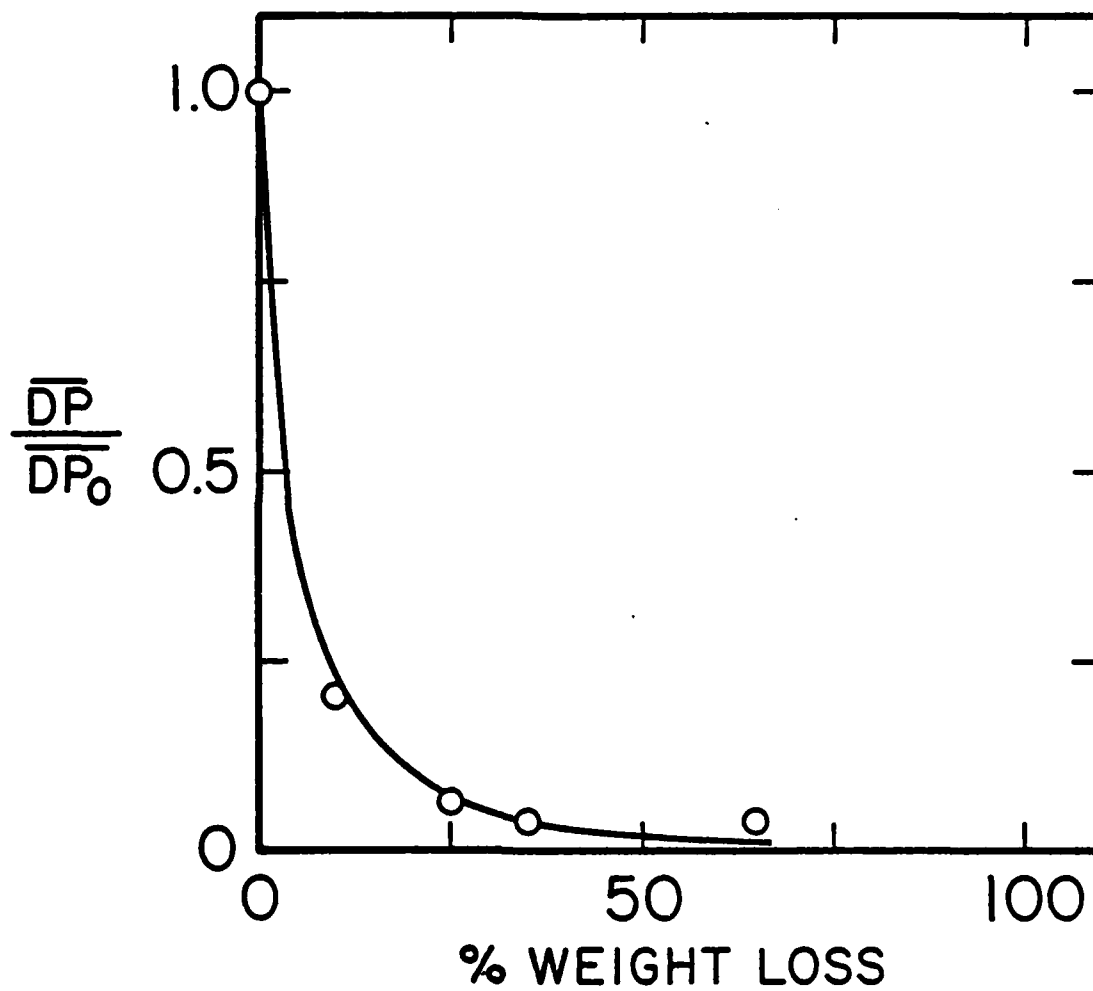


Figure 7. Relative molecular weight fraction ($\overline{DP}/\overline{DP}_0$) versus % weight loss (from ref. 9).

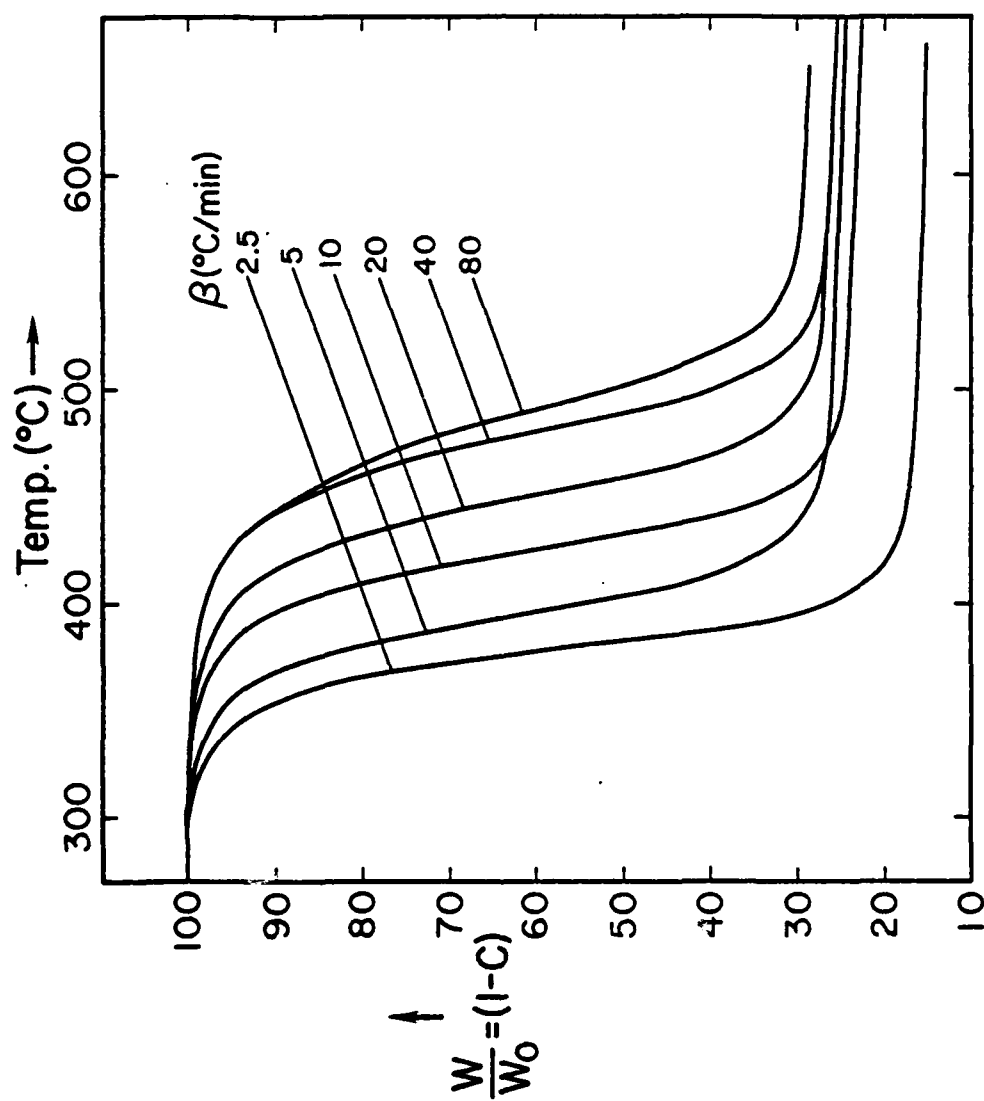


Figure 8. Percent weight loss ($l-C$) versus temperature ($^{\circ}\text{C}$) for PBPP specimens at different heating rates ($^{\circ}\text{C}/\text{min}$) from 2.5 to 80 $^{\circ}\text{C}/\text{min}$, in helium.

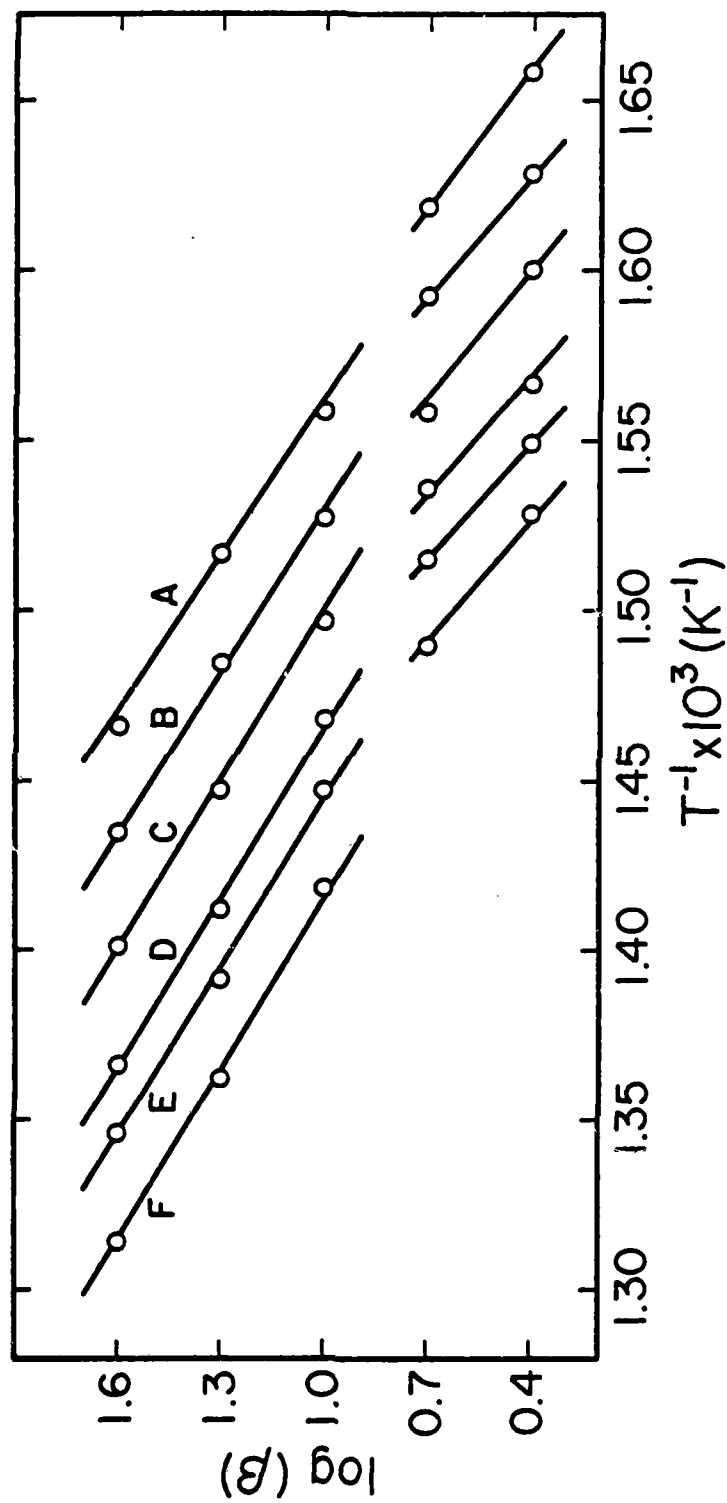


Figure 9. Long rate of heating β ($^{\circ}\text{C}/\text{min.}$) versus reciprocal temperature (K^{-1}) for the degradation of PBPP in helium for conversion levels: A 2.5%; B 5%; C 10%; D. 20%; E. 30%; F 50%.

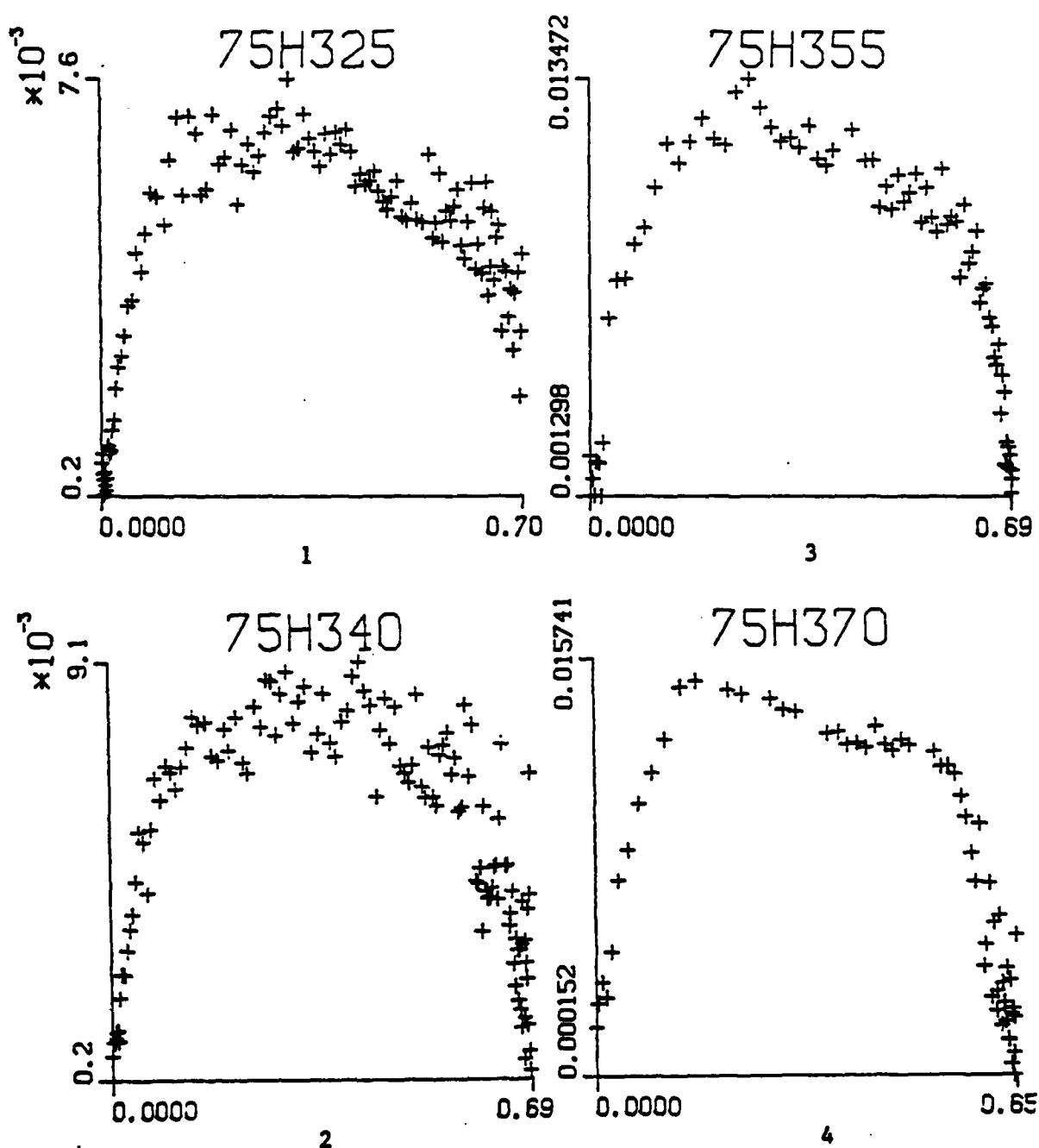


Figure 10. Rate of weight loss (min^{-1}) (based on residue) versus fractional conversion (abscissa) for isothermal degradation of PBPP in helium at: A 325°C; B 340°C; C 355°C; D 370°C. Data was computer digitized and plotted.

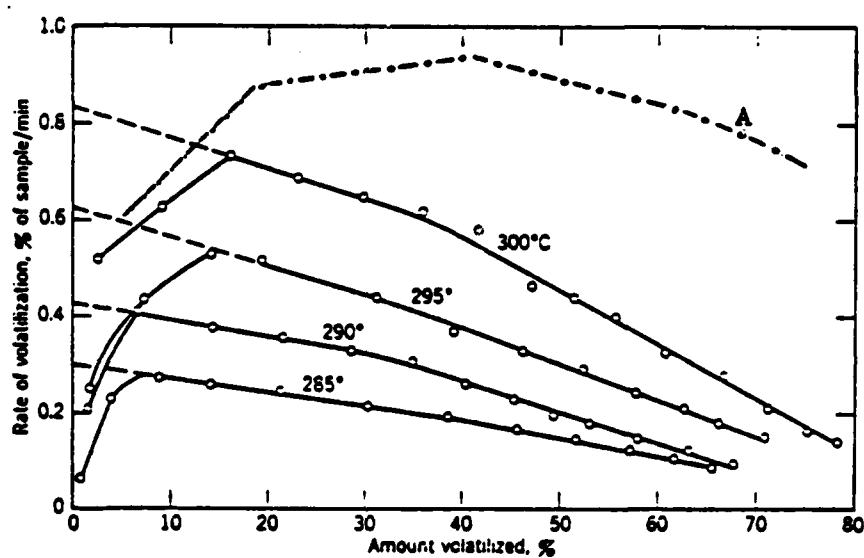


Figure 11. Rate of volatilization of isotactic polypropyleneoxide, (wt.% sample/min) versus amount volatilized, % (wt.%) at 285°, 290°, 295° and 300°C respectively (from ref. 20). Curve A is calculated from rate data (300°C) and represents the rate of weight loss (based on residue) as a function of sample volatilized. (Figure reproduced in part by permission).

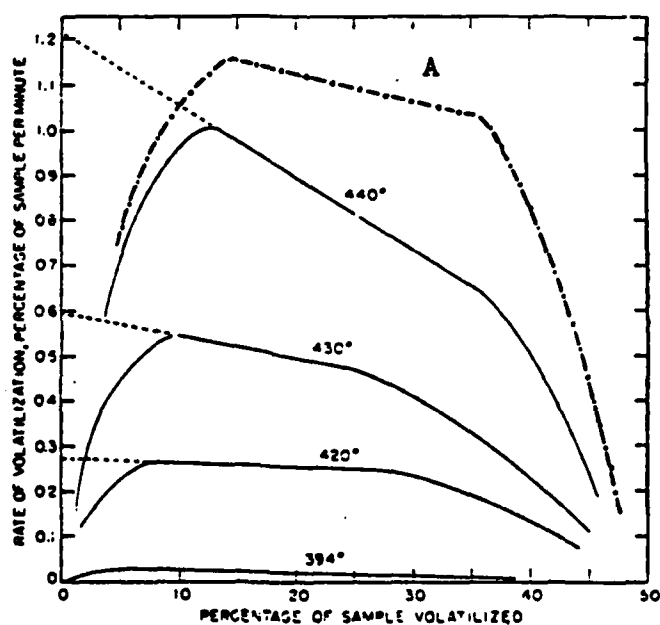


Figure 12. Rate of volatilization (wt. % per min.) of poly(trivinylbenzene) as a function of sample volatilized (wt. %) at 394°, 420, 430, and 440°C respectively (ref. 20). Curve A has been calculated from rate data at 440°C and depicts the rate of weight loss (based upon residue) as a function of sample volatilized (wt. %) (Figure reproduced in part by permission).

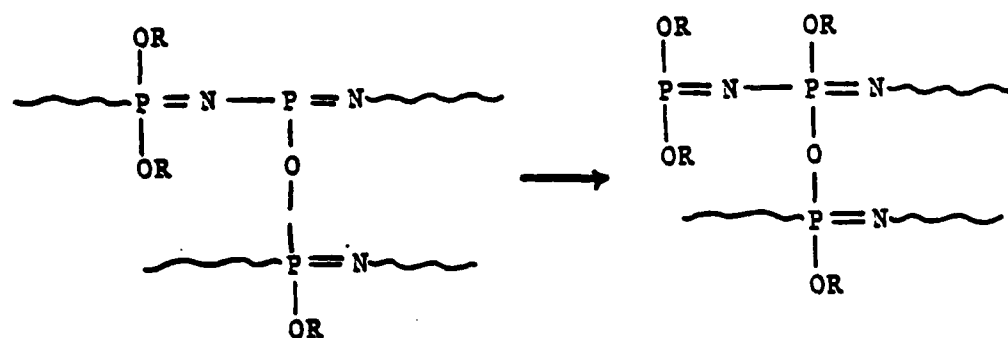


Figure 13. Schematic illustration of crosslinking in PBPP.

TECHNICAL REPORT DISTRIBUTION LIST, GEN

	<u>No.</u> <u>Copies</u>	
Office of Naval Research Attn: Code 472 800 North Quincy Street Arlington, Virginia 22217	2	U.S. Army Research Office Attn: CRD-AA-IP P.O. Box 1211 Research Triangle Park, N.C. 27709
ONR Branch Office Attn: Dr. George Sandoz 536 S. Clark Street Chicago, Illinois 60605	1	Naval Ocean Systems Center Attn: Mr. Joe McCartney San Diego, California 92152
ONR Branch Office Attn: Scientific Dept. 715 Broadway New York, New York 10003	1	Naval Weapons Center Attn: Dr. A. B. Amster, Chemistry Division China Lake, California 93555
ONR Branch Office 1030 East Green Street Pasadena, California 91106	1	Naval Civil Engineering Laboratory Attn: Dr. R. W. Drisko Port Hueneme, California 93401
ONR Branch Office Attn: Dr. L. H. Peebles Building 114, Section D 666 Summer Street Boston, Massachusetts 02210	1	Department of Physics & Chemistry Naval Postgraduate School Monterey, California 93940
Director, Naval Research Laboratory Attn: Code 6100 Washington, D.C. 20390	1	Dr. A. L. Slafkosky Scientific Advisor Commandant of the Marine Corps (Code RD-1) Washington, D.C. 20380
The Assistant Secretary of the Navy (R,E&S) Department of the Navy Room 4E736, Pentagon Washington, D.C. 20350	1	Office of Naval Research Attn: Dr. Richard S. Miller 800 N. Quincy Street Arlington, Virginia 22217
Commander, Naval Air Systems Command Attn: Code 310C (H. Rosenwasser) Department of the Navy Washington, D.C. 20360	1	Naval Ship Research and Development Center Attn: Dr. G. Bosmajian, Applied Chemistry Division Annapolis, Maryland 21401
Defense Documentation Center Building 5, Cameron Station Alexandria, Virginia 22314	12	Naval Ocean Systems Center Attn: Dr. S. Yamamoto, Marine Sciences Division San Diego, California 91232
Dr. Fred Saalfeld Chemistry Division Naval Research Laboratory Washington, D.C. 20375	1	Mr. John Boyle Materials Branch Naval Ship Engineering Center Philadelphia, Pennsylvania 19112

TECHNICAL REPORT DISTRIBUTION LIST, GEN

No.
Copies

Dr. Rudolph J. Marcus
Office of Naval Research
Scientific Liaison Group
American Embassy
APO San Francisco 96503

1

Mr. James Kelley
DTNSRDC Code 2803
Annapolis, Maryland 21402

1

TECHNICAL REPORT DISTRIBUTION LIST, 356B

	<u>No.</u> <u>Copies</u>	
Dr. T. C. Williams Union Carbide Corporation Chemical and Plastics Tarrytown Technical Center Tarrytown, New York	1	Douglas Aircraft Company 3855 Lakewood Boulevard Long Beach, California 90846 Attn: Technical Library CI 290/36-84 AUTO-Sutton
Dr. R. Soulen Contract Research Department Pennwalt Corporation 900 First Avenue King of Prussia, Pennsylvania 19406	1	NASA-Lewis Research Center 21000 Brookpark Road Cleveland, Ohio 44135 Attn: Dr. T. T. Serafini, MS 49-1
Dr. A. G. MacDiarmid University of Pennsylvania Department of Chemistry Philadelphia, Pennsylvania 19174	1	Dr. J. Griffith Naval Research Laboratory Chemistry Section, Code 6120 Washington, D.C. 20375
Dr. C. Pittman University of Alabama Department of Chemistry University, Alabama 35486	1	Dr. G. Goodman Globe-Union Incorporated 5757 North Green Bay Avenue Milwaukee, Wisconsin 53201
Dr. H. Allcock Pennsylvania State University Department of Chemistry University Park, Pennsylvania 16802	1	Dr. E. Fischer, Code 2853 Naval Ship Research and Development Center Annapolis Division Annapolis, Maryland 21402
Dr. M. Kenney Case-Western University Department of Chemistry Cleveland, Ohio 44106	1	Dr. Martin H. Kaufman, Head Materials Research Branch (Code 4542) Naval Weapons Center China Lake, California 93555
Dr. R. Lenz University of Massachusetts Department of Chemistry Amherst, Massachusetts 01002	1	
Dr. M. David Curtis University of Michigan Department of Chemistry Ann Arbor, Michigan 48105	1	Dr. C. Allen University of Vermont Department of Chemistry Burlington, Vermont 05401
Dr. M. Good Division of Engineering Research Louisiana State University Baton Rouge, Louisiana 70803	1	Dr. D. Bergbreiter Texas A&M University Department of Chemistry College Station, Texas 77843

TECHNICAL REPORT DISTRIBUTION LIST, 356B

No.
Copies

Professor R. Drago
Department of Chemistry
University of Illinois
Urbana, Illinois 61801 1

Dr. F. Brinkman
Chemical Stability & Corrosion
Division
Department of Commerce
National Bureau of Standards
Washington, D.C. 20234 1

Professor H. A. Titus
Department of Electrical Engineering
Naval Postgraduate School
Monterey, California 93940 1

COL B. E. Clark, Code 100M
Office of Naval Research
800 N. Quincy Street
Arlington, Virginia 22217 1

Professor T. Katz
Department of Chemistry
Columbia University
New York, New York 10027 1